Int. J. Heat Mass Transfer. Vol. 22, pp. 1033–1040
© Pergamon Press Ltd. 1979. Printed in Great Britain

0017-9310/79/0701-1033 $02.00/0

EFFECT OF INTERFACIAL PHENOMENA IN THE INTERLINE REGION ON THE REWETTING OF A HOT SPOT

P. C. WAYNER, JR.
Department of Chemical and Environmental Engineering, Rensselaer Polytechnic Institute,
Troy, N.Y. 12181, U.S.A.

(*Received* 16 *August* 1978 *and in revised form* 18 *January* 1979)

Abstract—The London–van der Waals dispersion force concept is used to analyze the interline region of a falling evaporating thin film. Viscous flow significantly affects the upstream profile, e.g. the apparent contact angle. The slope of the liquid–vapor interface is equal to a dimensionless interline heat sink. An increase in the apparent contact angle causes an increase in the rewetting velocity. Large interline temperature gradients and superheats are possible with either a stationary or moving interline. The physical process whereby the interline of a falling evaporating film can be in contact with a superheated surface is described.

NOMENCLATURE

$\bar{A}$,	dispersion constant [J];
c,	heat capacity $[\mathrm{J \cdot kg^{-1} K^{-1}}]$;
g,	gravitational acceleration $[\mathrm{m \cdot s^{-2}}]$;
H,	molar latent heat of vaporization $[\mathrm{J \cdot mol^{-1}}]$;
h_{fg},	latent heat of vaporization $[\mathrm{J \cdot kg^{-1}}]$;
k,	thermal conductivity of solid $[\mathrm{W \cdot m^{-1} \cdot K^{-1}}]$;
M,	molecular weight $[\mathrm{kg \cdot mol^{-1}}]$;
$\dot{m}$,	mass flux $[\mathrm{kg \cdot m^{-2} \cdot s^{-1}}]$;
P,	pressure $[\mathrm{N \cdot m^{-2}}]$;
Q,	heat flow rate $[\mathrm{W \cdot m^{-1}}]$;
q,	heat flux $[\mathrm{W \cdot m^{-2}}]$;
$\mathscr{R}$,	universal gas constant $[\mathrm{J \cdot mol^{-1} \cdot K^{-1}}]$;
T,	temperature [K];
t,	time [s];
U,	interline velocity $[\mathrm{m \cdot s^{-1}}]$;
u,	velocity $[\mathrm{m \cdot s^{-1}}]$;
V,	molar volume $[\mathrm{m^3 \cdot mol^{-1}}]$;
x,	coordinate length [m].

Greek symbols

Γ,	mass flowrate per unit width $[\mathrm{kg \cdot m^{-1}}]$;
δ,	film thickness [m];
ε,	lamina thickness [m];
ζ,	moving coordinate $x - Ut$ [m];
η,	dimensionless film thickness;
θ,	contact angle [deg];
μ,	absolute viscosity $[\mathrm{kg \cdot m^{-1} \cdot s^{-1}}]$;
ν,	kinematic viscosity $[\mathrm{m^2 \cdot s^{-1}}]$;
ρ,	density $[\mathrm{kg \cdot m^{-3}}]$;
Φ,	potential $[\mathrm{m^2 \cdot s^{-2}}]$;
Ω,	dimensionless interline heat sink.

Subscripts

d,	disjoining;
E,	excess;
e,	evaporative, apparent;
f,	fixed interline;
l,	liquid phase;
lv,	liquid–vapor interface;
M,	monolayer thickness;
m,	moving interline;
0,	evaluated at interline;
00,	equilibrium thin film;
s,	solid; saturation temperature;
t,	thermoosmotic;
v,	vapor phase;
w,	hot spot temperature;
x,	evaluated at x;
ζ,	evaluated at ζ.

Superscripts

id,	ideal;
$'$,	derivative with respect to x;
$*$,	derivative with respect to ζ;
$\bar{}$,	average.

INTRODUCTION

THE BEHAVIOR of the junction of an evaporating liquid film, the corresponding vapor, and the adsorbed, non-evaporating film on a solid is important to the understanding of many change of phase heat transfer processes (e.g. the rewetting of a hot spot, boiling and the evaporating meniscus). This junction is termed the interline and is particularly important because it is the junction between the evaporating and non-evaporating regions of the thin film. (Alternatively, the term contact line is used to designate the junction of the thin film with the vapor and "clean" solid surface.) In particular, the analysis presented below demonstrates that viscous flow in the vicinity of the interline significantly affects the rewetting velocity and the upstream profile of a falling evaporating thin film. Large interline superheats and temperature gradients are predicted.

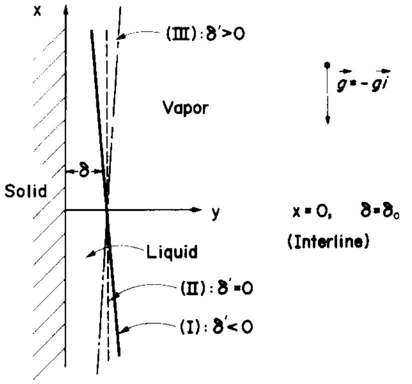

FIG. 1. Adsorbed thin film of liquid. Depending on the relative size of the temperature gradient, the slope δ' can be either $\delta' < 0$, $\delta' = 0$ or $\delta' > 0$.

The system to be studied consists of a thin, adsorbed film of pure liquid on a vertical flat solid surface (see Fig. 1). The analysis is restricted to non-polar liquids wetting the solid substrate in which the intermolecular interactions can be predicted from London's theory of dispersion forces. The liquid film and the solid substrate are assumed to be at a varying temperature above the saturation temperature of the liquid. If the film is sufficiently thin, it is kept from evaporating by the London–van der Waals dispersion force acting between the solid and liquid. Depending on the size and sign of the temperature gradient relative to the size and sign of the film thickness gradient, portions of the film may either be evaporating or not evaporating. The junction between these two regions is the interline $\delta = \delta_0$. Fluid flows in the negative "x" direction towards the interline as a result of gravity and/or a pressure gradient in the film arising from a film thickness gradient. In addition, the temperature gradient can either aid or impede the fluid flow.

The past literature in closely related areas is enormous and beyond the scope of this paper. However, it is desirable to relate the current work to the literature in two particularly relevant areas: the stability of a dry patch in a falling evaporating film and the rewetting of a hot spot. Norman and McIntyre [1] and Norman and Binns [2] discussed the effect of surface tension changes on the minimum wetting rate of a falling evaporating film. Hartley and Murgatroyd [3] modeled the effect of surface tension and contact angle on the break up of thin liquid films. These analyses were extended to include ebullition and thermocapillarity [4] and vapor thrust and thermocapillarity [5]. Extensive macroscopic experimental data and discussions of relevant models have been presented by various authors [e.g. 6–8]. In these references, the macroscopic contact angle and the liquid–vapor surface tension were used to describe the effect of interfacial forces on the transport processes. As outlined below, the microscopic nature of the interfacial forces necessitates a more detailed description of the transport processes in the interline region. In this vein, Ponter *et al.* [9] discussed the use of the London–van der Waals dispersion force concept. However, the lack of adequate models frustrated their efforts. A set of equations presented by Wayner *et al.* [10] for the interline region now makes it possible to use the London–van der Waals dispersion force concept to extend our understanding of transport processes in the interline region (film thickness less than approximately 10^{-7} m) where the thinness of the film obviates the need to separate the surface region from the bulk region. These equations are used herein to explain why the interline evaporation process is stable in the presence of large superheats and temperature gradients. The effect of interfacial forces on the transport processes is found to be enormous when the film thickness approaches that of a few monolayers. In addition, the apparent contact angle is found to be a function of the heat flux, the interline velocity and the optical and thermophysical properties of the system.

In the initial part of this paper, the equations are developed for a stationary interline. In the later part of this paper, the equations developed for the stationary interline are extended to apply to the problem of rewetting a hot spot which has also been extensively studied [e.g. 11–16]. However, these previous studies did not address the physics of the thin film transport processes in the interline region. Again, the use of the London–van der Waals dispersion force concept leads to enhanced understanding of heat transfer in the interline region.

INTERLINE CONDITIONS

The thermodynamic equation for the change in vapor pressure of an adsorbed non-evaporating thin film of liquid in equilibrium with its vapor is

$$\mathrm{d}\ln P_{vlv} = \frac{V_l}{\mathscr{R}T_l}\,\mathrm{d}P_l + \frac{H^{\mathrm{id}}}{\mathscr{R}T_l^2}\,\mathrm{d}T_l, \qquad (1)$$

where H^{id} is the "ideal" molar heat of vaporization for the liquid expanding into a vacuum. [The heat of vaporization for adsorbed films with thicknesses equal to that of a few monolayers and less is expected to be a function of the film thickness. Herein, this effect is presumed to be relatively small and of secondary importance. The significance of the final results and the conclusions are not believed to be effected by this presumption.] The effective pressure in the liquid, P_l, is less than the pressure in the vapor at the liquid–vapor interface, P_{vlv}, as a result of the London–van der Waals dispersion force of attraction between the solid and liquid. This difference can be related to the film thickness, δ_{00} in the equilibrium case, by the "disjoining pressure", P_d, [10, 17],

$$P_d = P_l - P_{vlv} = -\bar{A}\delta_{00}^{-n}, \qquad (2)$$

where $\bar{A}$ is a constant which accounts for the London–van der Waals force (the subscript $_{00}$ is used to designate the non-evaporating film). Using equation (1) the rate of change of the vapor pressure along the vertical liquid–vapor interface shown in Fig. 1 is

$$\frac{\mathrm{d}\ln P_{vlv}}{\mathrm{d}x}=\frac{V_l}{\mathscr{R}T_l}\frac{\mathrm{d}P_l}{\mathrm{d}x}-\frac{H^{\mathrm{id}}}{\mathscr{R}}\frac{\mathrm{d}T_l^{-1}}{\mathrm{d}x_l}. \tag{3}$$

Combining equations (2) and (3) and using $n = 3$ gives

$$\frac{\mathrm{d}\ln P_{vlv}}{\mathrm{d}x}$$
$$=\frac{V_l}{\mathscr{R}T_l}\left[\frac{\mathrm{d}P_{vlv}}{\mathrm{d}x}+\frac{3\bar{A}}{\delta_{00}^4}\frac{\mathrm{d}\delta_{00}}{\mathrm{d}x}\right]-\frac{H^{\mathrm{id}}}{\mathscr{R}}\frac{\mathrm{d}T_l^{-1}}{\mathrm{d}x}. \tag{4}$$

In the vapor space we have:

$$\frac{\mathrm{d}P_v}{\mathrm{d}x}=-\rho_v g, \tag{5}$$

or

$$\frac{\mathrm{d}\ln P_v}{\mathrm{d}x}=-\frac{Mg}{\mathscr{R}T_v}. \tag{6}$$

Using equations (4)–(6) with $P_v = P_{vlv}$ for the equilibrium case, the slope of the equilibrium liquid–vapor interface can be written as:

$$\frac{\mathrm{d}\delta_{00}}{\mathrm{d}x}=\frac{\delta_{00}^4}{3\bar{A}V_l}\left[\frac{Mg\rho_v}{\rho_l}-\frac{MgT_l}{T_v}-\frac{H^{\mathrm{id}}}{T_l}\frac{\mathrm{d}T_l}{\mathrm{d}x}\right]. \tag{7}$$

Therefore, depending on the size and sign of the temperature derivative, the slope of the equilibrium (non-evaporating) liquid–vapor interface can be either positive or negative.

For an evaporating thin film, equation (7) applies at the interline, i.e. where $\delta = \delta_0$. Hence,

$$\delta_0'=\frac{\delta_0^4}{3\bar{A}V_l}\left[\frac{Mg\rho_v}{\rho_l}-\frac{MgT_l}{T_v}-\frac{H^{\mathrm{id}}}{T_l}\frac{\mathrm{d}T_l}{\mathrm{d}x}\right], \tag{8}$$

where δ_0' is the slope of the film. Further, Wayner *et al.* [10] used equations (1) and (2) to obtain the film thickness boundary condition at the interline:

$$\delta_0=\left(\frac{\bar{A}V_lT_v}{H^{\mathrm{id}}(T_{lv}-T_v)}\right)_0^{1/3}. \tag{9}$$

Note that equation (7) also applies in the evaporating case for $\delta < \delta_0$ where the symbol δ_{0-} will be used for the non-evaporating region.

EVALUATION OF INTERLINE CONDITIONS

The following form of equation (9) is presented in Fig. 2:

$$\ln\frac{(\Delta T)_0}{T_{v0}}=\ln\frac{\bar{A}V_l}{H^{\mathrm{id}}}+\ln\delta_0^{-3}. \tag{10}$$

The relative size of the interline superheat, $(\Delta T)_0 = (T_{lv} - T_v)_0$, is a function of the dimensionless group $\bar{A}V_l/H^{\mathrm{id}}\delta_0^3$. Using nanometers, the vertical axis at $\delta_0 = 1$ nm (approximately 2–3 monolayers) can be used to list approximate values of $\bar{A}V_l/H^{\mathrm{id}}$ for various systems. Values for $\bar{A}$ were obtained from [18] where a procedure to determine the interline heat transfer characteristics from the macroscopic optical and thermophysical properties of the system is outlined.

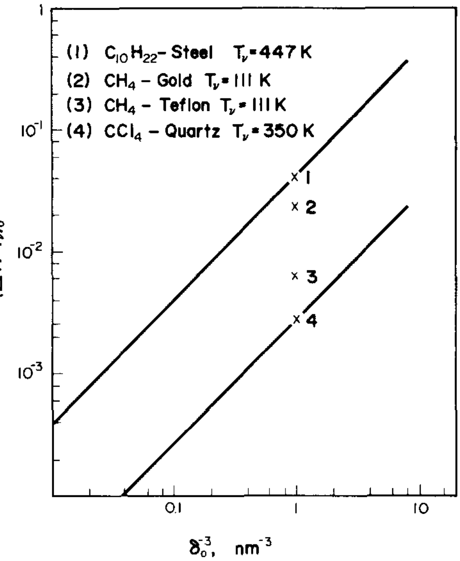

FIG. 2. Estimated values of the interline superheat, equation (10).

Bulk values were used for V_l and $H^{\mathrm{id}} \approx Mh_{fg}$. The most significant aspect of these results is the large predicted superheats for very thin films on clean surfaces. The possible superheats are still large for thicker films on less ideal surfaces. Therefore, this model describes a mechanism whereby thin evaporating stable films can easily stay in contact with superheated surfaces.

Table 1. $\left[\frac{\mathrm{d}\delta_0/\mathrm{d}x}{\mathrm{d}T_l/\mathrm{d}x}\right]\times 10^{10}\,\mathrm{m\,K^{-1}}$

	$\delta_0 = 10^{-9}$ m	$\delta_0 = 4\times10^{-9}$ m
$C_{10}H_{22}$-Steel		
T_l = 293K	−0.30	−76
T_l = 447K	−0.19	−48
CCl_4-Quartz		
T_l = 293K	−13.0	−3300
T_l = 350K	−3.5	−904

Equation (8) is presented in Table 1 for various film thicknesses and two values of the group $H^{\mathrm{id}}/3\bar{A}V_lT_l$. For the range of values presented, the effect of gravity on the slope is much smaller than the effect of the temperature gradient. These results predict that the interline slope (approximate real contact angle) is very small for wetting films even with very large temperature gradients. Again, the presence of a stable non-isothermal, non-evaporating, film is demonstrated. However, as described below, a small rate of evaporation will cause a significant change in the slope and, therefore, in the apparent contact angle.

FALLING EVAPORATING THIN FILM, STATIONARY INTERLINE

Using equation (7) we can predict that evaporation or condensation will occur at the surface of the thin film when

$$\frac{3\bar{A}}{\delta^4}\frac{\mathrm{d}\delta}{\mathrm{d}x}+g\left[\frac{\rho_l T_l}{T_v}-\rho_v\right]+\frac{H^{\mathrm{id}}}{V_l T_l}\frac{\mathrm{d}T_l}{\mathrm{d}x}\neq 0. \tag{11}$$

For a falling thin film, the small increase in slope at $\delta \gtrsim \delta_0$ above its equilibrium value which allows evaporation results from the weight of the thicker upstream film. As demonstrated below, a small increase in slope leads to significant evaporation and a significant change in the film profile in the region $\delta > \delta_0$.

Under the influence of a potential gradient, the velocity distribution at any point in the slightly tapered thin film, assuming a continuum, is obtained from the momentum equation:

$$\frac{\mathrm{d}\Phi_E}{\mathrm{d}x}=\mu\frac{\mathrm{d}^2 u}{\mathrm{d}y^2}, \tag{12a}$$

where the potential gradient results from the disjoining pressure gradient, gravity, and a thermoosmotic pressure gradient, P_t'.

$$\frac{\mathrm{d}\Phi_E}{\mathrm{d}x}=\frac{3\bar{A}\delta'}{\delta^4}+g(\rho_l-\rho_v)+P_t'. \tag{12b}$$

The boundary conditions are taken to be the traditional no-slip condition at the liquid–solid interface and the no-shear condition at the liquid–vapor interface. For these boundary conditions the mass flow rate per unit width of film is

$$\Gamma=-\frac{\delta^3\rho_l}{3\nu}\frac{\mathrm{d}\Phi_E}{\mathrm{d}x}. \tag{13}$$

Combining equations (12b) and (13) gives

$$-\Gamma=\frac{\bar{A}\delta'}{\nu\delta}+\frac{\delta^3 g}{3\nu}(\rho_l-\rho_v)+\frac{\delta^3}{3\nu}P_t'. \tag{14}$$

The evaporative mass flux leaving the film surface is obtained from equation (14) as

$$\dot{m}_e=-\frac{\mathrm{d}\Gamma}{\mathrm{d}x}. \tag{15}$$

The local heat flux $(\dot{m}_e h_{fg})$ is

$$q(x)=\frac{\mathrm{d}}{\mathrm{d}x}\left[\frac{\bar{A}h_{fg}\delta'}{\nu\delta}+\frac{gh_{fg}\delta^3}{3\nu}(\rho_l-\rho_v)+\frac{h_{fg}\delta^3}{3\nu}P_t'\right]. \tag{16}$$

The heat flow rate per unit width of film for the length x is termed the "interline heat sink", Q_f. Clearly

$$Q_f(x)=\int_0^x q(x)\,\mathrm{d}x. \tag{17}$$

Combining (16) and (17) gives

$$Q_f(x)=\left[\frac{\bar{A}h_{fg}\delta'}{\nu\delta}+\frac{gh_{fg}\delta^3}{3\nu}(\rho_l-\rho_v)+\frac{h_{fg}\delta^3}{3\nu}P_t'\right]_0^x. \tag{18}$$

This leads to the following approximate value of the interline heat sink:

$$Q_f(x)=\frac{\bar{A}h_{fg}\delta'(x)}{\delta(x)\nu}+\frac{gh_{fg}\delta^3(x)}{3\nu}(\rho_l-\rho_v). \tag{19}$$

The boundary condition at the interline is achieved by using a thermoosmotic effect in the model to offset the terms δ_0 and δ_0' which do not vanish. Alternatively, contact line motion occurs or a model which includes surface diffusion has to be used in the region $\delta_0 \to 0$. Further, the magnitudes of these terms are small at $x = 0$. At x, the thermoosmotic effect is very small, since the absolute magnitude of the temperature gradient decreases as x increases. The relative size of the gravitational term in (19) is small when δ is small. For this case, the effect of evaporation on the slope can be easily evaluated using equation (20).

$$\frac{\mathrm{d}\delta}{\mathrm{d}x}=\frac{Q_f\delta_0\nu\eta}{\bar{A}h_{fg}}=\Omega_f. \tag{20}$$

Equation (20) equates the slope at $\eta = \delta/\delta_0$ to the dimensionless interline heat sink Ω_f for the region $x > 0$. The thickness η can be obtained as a function of the length x [10, 19].

APPARENT CONTACT ANGLE, STATIONARY INTERLINE

Using equation (20) the apparent contact angle is given by

$$\theta_e=\tan^{-1}\left(\frac{Q_f\delta\nu}{\bar{A}h_{fg}}\right)_x. \tag{21}$$

In Fig. 3 the apparent contact angle at $\delta = 500$Å is presented as a function of the interline heat sink Q_f for the following two systems: CCl_4–Quartz (350K) and $C_{10}H_{22}$–Steel (447K). These results demonstrate that the apparent contact angle is a function of the interline heat sink and the properties of the system represented by the interline heat flow number $h_{fg}\bar{A}/\nu$. The apparent contact angle is an inverse measure of the heat sink capability of the interline region. Therefore, the interline heat sink capability of a simple fluid on metal is greater than that of a simple fluid on glass because the London–van der Waals dispersion force in the metal–fluid system is greater than that in the glass–fluid system. As in any

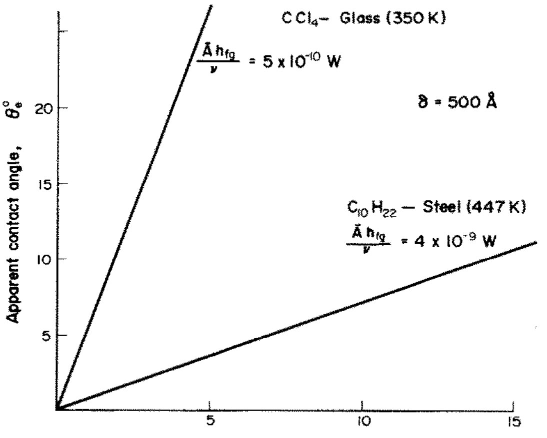

FIG. 3. Apparent contact angle at $\delta = 500$Å.

experimental system the point at which the contact angle is measured is arbitrary and depends on the resolution of the optical equipment. However, the real contact angle for these two systems is essentially zero as was detailed in the previous section [equation (8)].

FALLING EVAPORATING THIN FILM, MOVING INTERLINE

A mass balance for a differential segment of the film gives

$$\frac{\partial(\rho_l \bar{u}\delta)}{\partial x} + \frac{\partial(\rho_l \delta)}{\partial t} + \dot{m}_e = 0. \tag{22}$$

Using equation (23) for the average velocity in a thin film,

$$\bar{u} = -\frac{\delta^2}{3\mu}\frac{\partial P}{\partial x}, \tag{23}$$

and equation (12b) gives

$$\frac{\partial}{\partial x}\left[\frac{\bar{A}\delta'}{v\delta}\right] - \rho_l \frac{\partial \delta}{\partial t} - \dot{m}_e = 0. \tag{24}$$

Gravitational and thermo-osmotic effects are relatively small and, therefore, neglected in equation (24). For a thin film of a given shape moving at a constant velocity U we use the new variable $\zeta = x - Ut$, so that equation (24) is transformed to

$$\frac{\mathrm{d}}{\mathrm{d}\zeta}\left[\frac{\bar{A}\delta^*}{v\delta}\right] + \rho_l U \frac{\mathrm{d}\delta}{\mathrm{d}\zeta} - \dot{m}_e = 0. \tag{25}$$

Integrating equation (25) between $\zeta = 0$, where $\Gamma(0) = -\bar{A}\delta_0^*/v\delta_0 = \frac{2}{3}\rho_l U \delta_0$ and ζ gives

$$\frac{\bar{A}\delta^*}{v\delta} = \bar{\dot{m}}_e \zeta + \rho_l U\left(\frac{\delta_0}{3} - \delta\right). \tag{26}$$

Using equation (26) and $Q_m = h_{fg}\bar{\dot{m}}_e\zeta$ gives equation (27) for the slope of the liquid–vapor interface at ζ.

$$\delta^* = \frac{v\delta}{\bar{A}h_{fg}}\left[Q_m + \rho_l U h_{fg}\left(\frac{\delta_0}{3} - \delta\right)\right]. \tag{27}$$

Therefore, for a given heat flow rate Q_m an increase in the slope at ζ from the value given by equation (20) leads to interline motion with a velocity U. The increase in slope results from the weight of the thicker upstream film. The apparent conflict between a constant velocity and $\delta \to 0$ will be discussed below.

Using an energy balance for the heat loss per unit time from a very thin solid lamina of thickness ε being cooled from T_w to T_s to approximate the value of $\bar{\dot{m}}_e h_{fg}\zeta$ leads to equations (28) and (29) [see e.g. 15]:

$$\bar{\dot{m}}_e h_{fg}\zeta = \int_0^{\varepsilon}\int_{-\infty}^{\infty} \rho_s c_s\left(-\frac{\partial T}{\partial t}\right)\mathrm{d}x\,\mathrm{d}y \tag{28}$$

$$\bar{\dot{m}}_e h_{fg}\zeta = \rho_s c_s U\varepsilon(T_s - T_w). \tag{29}$$

Combining equations (26) and (29) and solving for the velocity results in:

$$U = \frac{-\dfrac{\delta^*\bar{A}}{v\delta}}{\left[\rho_l\left(\rho - \dfrac{\delta_0}{3}\right) + \rho_s c_s \varepsilon(T_w - T_s)/h_{fg}\right]}. \tag{30}$$

Equation (30) shows why, from an interline fluid mechanics point of view, an increase in slope and/or a decrease in $(T_w - T_s)$ leads to an increase in the absolute magnitude of the velocity for the rewetting of a hot spot.

The rewetting velocity given by equation (30) was obtained using interline fluid mechanics. For completeness this can be related to the following simplified equation in the literature for the film velocity which was obtained using a conduction controlled rewetting model [e.g. 15]:

$$U = \left(\frac{kh}{\varepsilon\rho_s^2 c_s^2}\right)^{1/2}\left(\frac{T_s - T_0}{T_w - T_0}\right). \tag{31}$$

The slope δ^* can be viewed as causing the mass flow rate close to the interline required by equation (31). It should be noted that the thickness of the lamina, ε, in equation (31) is much larger than the lamina thickness in equation (30) because of the relative size of regions modeled.

Using equations (20) and (27) gives:

$$\frac{\delta^*}{\delta'} = \frac{Q_m + \rho_l U h_{fg}\left(\dfrac{\delta_0}{3} - \delta\right)}{Q_f}, \tag{32}$$

for the relative increase in the slope with movement of the interline. The approximate values of Q_m and Q_f can be obtained from a one dimensional analysis of conduction controlled rewetting [15].

MOTION WHERE $\delta \to$ MONOLAYER

Considerable research has been done concerning the "slip velocity" associated with a moving contact line [20–24]. For example, Ruckenstein and Dunn have demonstrated that "a slip velocity at the contact line of a liquid on a solid surface originates because of the force induced by the gradient of the chemical potential in the liquid along the solid–liquid interface" [20]. The potential gradient for flow in the present paper is based on the same physical principle. Strictly speaking the use of a continuum approach is not entirely valid where the thickness is of molecular dimensions. However, the chemical potential gradient in the region where $\delta \to \delta_M$ can be sufficiently large so that it easily causes contact line motion whatever the velocity distribution. In addition, the error associated with using a parabolic velocity profile would not significantly effect the present results. As demonstrated by equations (8) and (10) the use of a model based on chemical potential also leads to the prediction of large superheats and large temperature gradients in the interline region.

APPARENT CONTACT ANGLE, MOVING INTERLINE

By neglecting the relatively small term $[\rho_l U(\delta_0/3 - \delta)]$ in equation (26) when $Q_m = h_{fg}\bar{m}\zeta$ is substantial, we can easily estimate the effect of evaporation on the moving contact angle evaluated at $\delta(\zeta)$:

$$\delta^* = \left(\frac{Q_m \nu \delta}{\bar{A} h_{fg}}\right)_\zeta . \tag{33}$$

Although equations (20) and (33) are of the same form, $\delta^* > \delta'$ at a given δ because $Q_m > Q_f$. The results presented in Fig. 3 apply to both cases.

Using a constant heat flux model for the moving interline region [19], $Q_m = \bar{q}_m \zeta$ and $\zeta = (2h_{fg}\bar{A} \ln \eta/\bar{q}_m \nu)^{0.5}$, gives

$$\delta^* = \left[\frac{2\bar{q}_m \eta^2 \delta_0^2 \ln \eta}{h_{fg}\bar{A}/\nu}\right]^{0.5}_\zeta . \tag{34}$$

Taking the ratio of equation (34) to a similar equation for a fixed interline [19] while keeping the dimensionless thickness η the same (note: when equations (20) and (33) were compared above, δ was kept constant) results in:

$$\frac{\delta^*}{\delta'} = \frac{\delta_{0m}}{\delta_{0f}} \left(\frac{\bar{q}_m}{\bar{q}_f}\right)^{0.5} . \tag{35}$$

Equations (35) emphasizes the controlling importance of the interline thickness δ_0. As a numerical example, we can focus on the decane-steel system presented in Fig. 3. Using these results, we can see that an order of magnitude increase in the moving interline heat sink above the fixed interline heat sink for the same dimensionless thickness change η would result in too large an increase in the contact angle unless a compensating decrease in the interline thickness occurred. The results presented above, equation (9), demonstrate that the interline thickness is a function of the interline temperature and, therefore, a decrease in interline thickness is expected with increased heat flux and interline motion. Although the calculation of exact values is beyond the scope of this paper, the results presented in Fig. 2 demonstrate that large changes in δ_0 can occur as a result of large changes in the interline temperature T_0. In addition, the results presented in Fig. 3 also apply to the moving interline case. However, an analysis of micro-conduction in the interline region is needed to obtain a detailed description of the effect of evaporation on the interline temperature, the interline thickness and, therefore, the contact angle for a specific case.

Since the interfacial heat transfer coefficient is huge for $\eta > 2$, small temperature increases in the region where $\eta > 2$ result in large changes in the evaporative heat sink [10]. Therefore, the major resistance to heat flow is in the solid where large variations in the temperature gradient are needed. The above analysis demonstrates that the interfacial forces are sufficient to maintain a stable (moving or stationary) interline with a substantial temperature gradient in the solid and a large interline superheat.

DISCUSSION

Although many simplifying assumptions were used in the above analysis, a useful procedure has been developed to analyze the interline region. The significance of these results is that they describe the physical process whereby the interline of a falling evaporating film can be in contact with a hot surface. The results agree with the following experimentally observed phenomena: the apparent contact angle of an evaporating meniscus is a function of the heat flux [25]; the interline temperature of a rewetting film is significantly above the saturation temperature, and the temperature gradient in the interline region is very large [11–13]; the rewetting velocity can be a function of the surface characteristics [14]; and the value of the apparent contact angle at a dry spot is a function of the heat flux [7]. I hasten to point out that these experimental observations are not presented as direct experimental verification of the above analysis because of the presence within them of many conflicting phenomena. It should be further noted that the analysis was directed at a wetting system (contact angle of zero) although the predicted trends should hold for the non-wetting experimental systems referred to. The above results can be used to design experiments with the necessary restraints to alleviate these uncertainties.

CONCLUSIONS

The analysis leads to the following conclusions:

1. At the interline of a falling evaporating film in a liquid–solid system which has an isothermal contact angle equal to zero, the real contact angle is very small and is a function of the temperature gradient and the interline velocity.
2. Large superheats and extremely large temperature gradients in the interline region of a stable evaporating thin film are thermodynamically possible.
3. Viscous flow of the evaporating liquid in the interline region has a significant effect on the apparent (observable) contact angle.
4. The apparent contact angle of an evaporating film is significantly different from the real contact angle.
5. An increase in the apparent contact angle gives an increase in the rewetting velocity.
6. The interline velocity of an evaporating film is a function of the heat flux, the apparent contact angle, and the optical and thermophysical properties of the solid–liquid system.
7. The apparent contact angle can be expressed as a function of a dimensionless interline heat sink, $\delta Q \nu / h_{fg}\bar{A}$.
8. The interline heat sink capability of a simple fluid on metal is greater than that of a simple fluid on glass because the London–van der Waals dispersion force in the metal–fluid system is greater than that in the glass fluid system.

Acknowledgement—I gratefully acknowledge the financial support of NSF Grant ENG 76-01608.

REFERENCES

1. W. S. Norman and V. McIntyre, Heat transfer to a liquid film on a vertical surface, *Trans. Instn Chem. Engrs* **38**, 301–307 (1960).
2. W. S. Norman and D. T. Binns, The effect of surface tension changes on the minimum wetting rates in a wetted-rod distillation column, *Trans. Instn Chem. Engrs* **38**, 294–300 (1960).
3. D. E. Hartley and W. Murgatroyd, Criteria for the break-up of thin liquid layers flowing isothermally over solid surfaces, *Int. J. Heat Mass Transfer* **7**, 1003–1015 (1964).
4. Y. Y. Hsu, F. F. Simon and J. F. Lad, Destruction of a thin liquid film flowing over a heating surface, *Chem. Engng Prog. Symp. Ser.* **61**(57), 139–152 (1965).
5. N. Zuber and F. W. Staub, Stability of dry patches forming in liquid films flowing over heated surfaces, *Int. J. Heat Mass Transfer* **9**, 897–905 (1966).
6. G. D. McPherson, Axial stability of the dry patch formed in dryout of a two-phase annular flow, *Int. J. Heat Mass Transfer* **13**, 1133–1152 (1970).
7. A. Orell and S. G. Bankoff, Formation of a dry spot in a horizontal liquid film heated from below, *Int. J. Heat Mass Transfer* **14**, 1835–1842 (1971).
8. T. Fujita and T. Ueda, Heat transfer to falling liquid films and film breakdown, *Int. J. Heat Mass Transfer* **21**, 97–118 (1978).
9. A. B. Ponter, G. A. Davies, W. Beaton and T. K. Ross, The measurement of contact angles under conditions of heat transfer when a liquid film breaks on a vertical surface, *Int. J. Heat Mass Transfer* **10**, 1633–1636 (1967).
10. P. C. Wayner, Jr., Y. K. Kao and L. V. LaCroix, The interline heat-transfer coefficient of an evaporating wetting film, *Int. J. Heat Mass Transfer* **19**, 487–492 (1976).
11. R. Semeria and B. Martinet, Calefaction spots on a heating wall: temperature distribution and resorption, *Proc. Symp. Boiling Heat Transfer in Steam-Generating Units and Heat Exchangers* **180**(3C), Manchester Sept. 15–16 (1965).
12. T. S. Thompson, An analysis of the wet-side heat-transfer coefficient during rewetting of a hot dry patch, *Nucl. Engng Des.* **22**, 212–224 (1972).
13. A. W. Bennett, G. F. Hewitt, H. A. Kearsey and R. K. F. Keeys, The wetting of hot surfaces by water in a steam environment at high pressure, AERE-R5146 (1966).
14. B. D. G. Piggott and R. B. Duffey, The quenching of irradiated fuel pins, *Nucl. Engng Des.* **32**, 182–190 (1975).
15. R. B. Duffey and D. T. C. Porthouse, The physics of rewetting in water reactor emergency core cooling, *Nucl. Engng Des.* **25**, 379–394 (1973).
16. A. Yamanouchi, Effect of core spray cooling in transient state after loss of coolant accident, *J. Nucl. Sci. Tech.* **5**, 547–588 (1968).
17. B. V. Deryagin and A. M. Zorin, Optical study of the adsorption and surface condensation of vapors in the vicinity of saturation on a smooth surface, *Proc. 2nd Int. Congr. Surface Activity* (*Lond.*) **2**, 145–152 (1957).
18. P. C. Wayner, Jr., The effect of the London–van der Waals dispersion force on interline heat transfer, *Trans. ASME, J. Heat Transfer* **100**, 155–159 (1978).
19. P. C. Wayner, Jr., A constant heat flux model of the evaporating interline region, *Int. J. Heat Mass Transfer* **21**, 362–364 (1978).
20. E. Ruckenstein and C. S. Dunn, Slip velocity during wetting of solids, *J. Colloid Interface Sci.* **59**, 135–138 (1977).
21. E. B. Dussan and S. H. Davis, On the motion of a fluid–fluid interface along a solid surface, *J. Fluid Mech.* **65**, 71–95 (1974).
22. C. A. Miller and E. Ruckenstein, The origin of flow during wetting of solids, *J. Colloid Interface Sci.* **48**, 368–373 (1974).
23. C. Huh and L. E. Scriven, Hydrodynamic model of steady movement of a solid/liquid/fluid contact line, *J. Colloid Interface Sci.* **35**, 85–101 (1971).
24. V. Ludviksson and E. N. Lightfoot, Deformation of advancing menisci, *A.I.Ch.E. J.* **14**, 674–677 (1968).
25. F. J. Renk and P. C. Wayner, Jr., An evaporating ethanol meniscus: Part I, Experimental studies, *J. Heat Transfer* **101C**, 55–58 (1979).

EFFET DU PHENOMENE INTERFACIAL SUR LE REMOUILLAGE D'UN POINT CHAUD DANS LA REGION DE LA LIGNE SEPARATION

Résumé Le concept de la force de dispersion de London–Van der Waals est utilisé pour analyser la région frontière d'un film mince tombant et s'évaporant. L'écoulement visqueux affecte sensiblement le profil amont et l'angle apparent de contact. La pente de l'interface liquide–vapeur est égale à un puits de chaleur adimensionnel à l'interligne. Un accroissement de l'angle apparent de contact cause un accroissement de la vitesse de remouillage. De grands gradients de température à l'interligne et de fortes surchauffes sont possibles aussi bien avec l'interligne stationnaire que mobile. On décrit le mécanisme physique par lequel l'interligne d'un film tombant et s'évaporant peut être en contact avec une surface surchauffée.

DER EINFLUSS VON GRENZFLÄCHEN-ERSCHEINUNGEN IM GRENZLINIEN-GEBIET AUF DIE WIEDERBENETZUNG EINER HEISSEN STELLE

Zusammenfassung—Das Konzept der London-van der Waals'schen Dispersionskräfte wird zur Analyse des Grenzlinien-Gebiets eines fallenden, verdampfenden, dünnen Films herangezogen. Zähigkeitsglieder beeinflussen maßgeblich das stromaufwärts liegende Strömungsprofil, also den scheinbaren Randwinkel. Die Steigung der Flüssigkeits-Dampf-Grenzfläche ist gleich einer dimensionslosen Grenzlinien-Wärmesenke. Eine Zunahme des scheinbaren Randwinkels bewirkt eine Zunahme der Wiederbenetzungs-Geschwindigkeit. Große Grenzlinien-Temperaturgradienten und Überhitzungen sind sowohl bei ortsfester wie auch bei wandernder Grenzlinie möglich. Der physikalische Prozeß, bei dem die Grenzlinie eines fallenden, verdampfenden Films in Kontakt mit einer überhitzten Oberfläche sein kann, wird beschrieben.

ВЛИЯНИЕ МЕЖФАЗНЫХ ЯВЛЕНИЙ В ОБЛАСТИ ГРАНИЦЫ РАЗДЕЛА НА ПОВТОРНОЕ СМАЧИВАНИЕ ЗОНЫ ПЕРЕГРЕВА

Аннотация — В статье используется понятие о дисперсионных силах Лондона-Ван дер Ваальса для анализа граничной области стекающей испаряющейся тонкой пленки жидкости. Вязкость потока оказывает значительное влияние на профиль вверх по течению, например, на угол контакта. Наклон границы раздела жидкость-пар равен безразмерному стоку тепла на границе пленки. Увеличение угла контакта вызывает увеличение скорости смачивания. Большие температурные градиенты на границе пленки и перегревы могут иметь место как для неподвижной, так и для движущейся плёнки. Описывается физический процесс на границе контакта стекающей испаряющейся плёнки с поверхностью перегрева.